Nanoscale RSCPublishing

Supporting Information

Metal nanocluster light-emitting devices with suppressed parasitic emission and improved efficiency: Exploring the impact of photophysical properties

T. –W. Koh,[a] A. M. Hiszpanski,[b] M. Sezen,[b] A. Naim,[c] T. Galfsky,[c] A. Trivedi,[d] Y. –L. Loo,[b] V. Menon[c] and B. P. Rand[a,e]

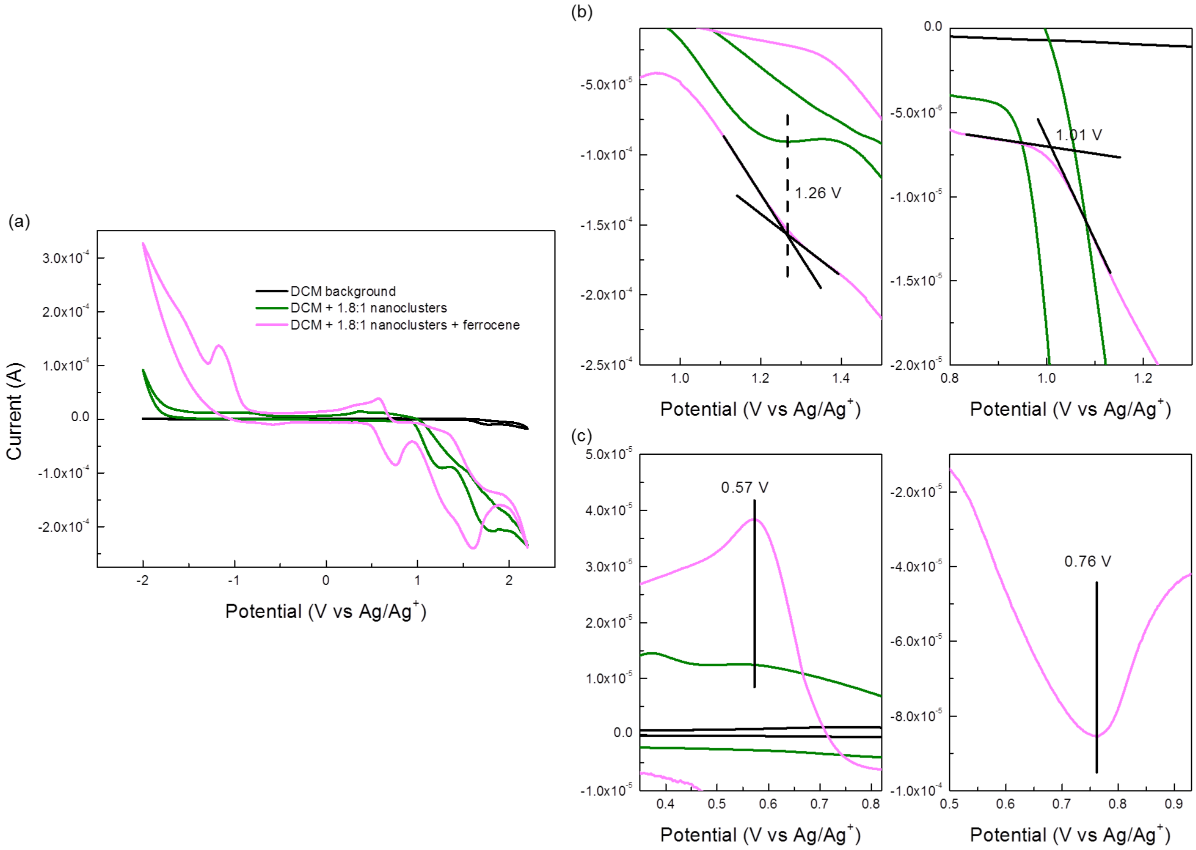

Figure S1. (a) Cyclic voltammograms for three solutions: dichloromethane (DCM) with tributylammonium hexafluorophosphate (shown as DCM background, black line), with 1.8:1 nanocluster added (green line), and with ferrocene added as an internal reference (light magenta line). A reductive peak at ca. -1 V vs. Ag/Ag+ appears upon the addition of ferrocene to the nanocluster solution, which is present upon repeated cycling and appears across samples (see Figure S2). We note that the peak is not present in scans of only ferrocene or only nanoclusters. However, this reduction event does not appear to affect the oxidation events (and thus the extracted HOMO energy levels) of the nanoclusters as the oxidative half-potentials of the nanoclusters do not change significantly upon the addition of ferrocene. (b)

Zoomed-in views of the oxidation peaks from the nanoclusters in the two solutions (DCM + nanocluster (green), DCM + nanocluster + ferrocene (light magenta)). The oxidation half-potential of the nanoclusters is (1.26+1.01)/2 = 1.135 V vs. Ag/Ag$^+$. (c) Zoomed-in views of the oxidation peaks from ferrocene. The oxidative half-potential of ferrocene is (0.57+0.76)/2 = 0.665 V vs. Ag/Ag+. Given that the HOMO of ferrocene is 4.8 eV and that the difference between the oxidative half-potentials of the nanoclusters and the ferrocene is 1.135-0.665 = 0.47 V, the HOMO level of the nanocluster can be estimated to be 4.8+0.47 = 5.27 eV. All plots are plotted following the IUPAC convention.

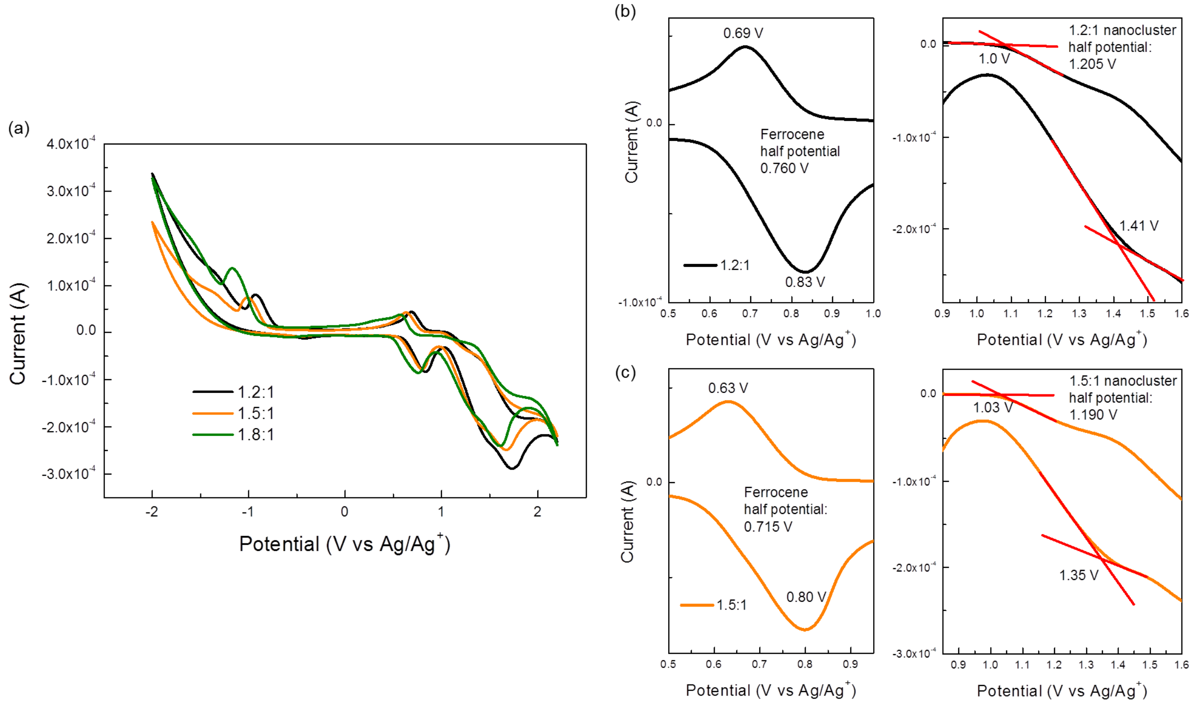

Figure S2. (a) Cyclic voltammograms of three different nanocluster solutions with various GSH:Au salt ratios. (b) Oxidation peaks from the ferrocene standard (left) and 1.2:1 nanoclusters (right) giving oxidation half-potentials of 0.76 and 1.21 V vs. Ag/Ag^+, respectively. Given that the difference in their oxidative half-potentials is 1.21-0.76 = 0.45 V, the nanoclusters' HOMO level is estimated as 4.8+0.45 = 5.25 eV. (c) Oxidation peaks from the ferrocene standard (left) and 1.5:1 nanoclusters (right) yielding oxidation half-potentials of 0.715 and 1.19 V vs. Ag/Ag^+, respectively. Given that the difference in their oxidative half-potentials is 1.19-0.715 = 0.475 V, the nanoclusters' HOMO level is estimated as 4.8+0.475 = 5.28 eV.

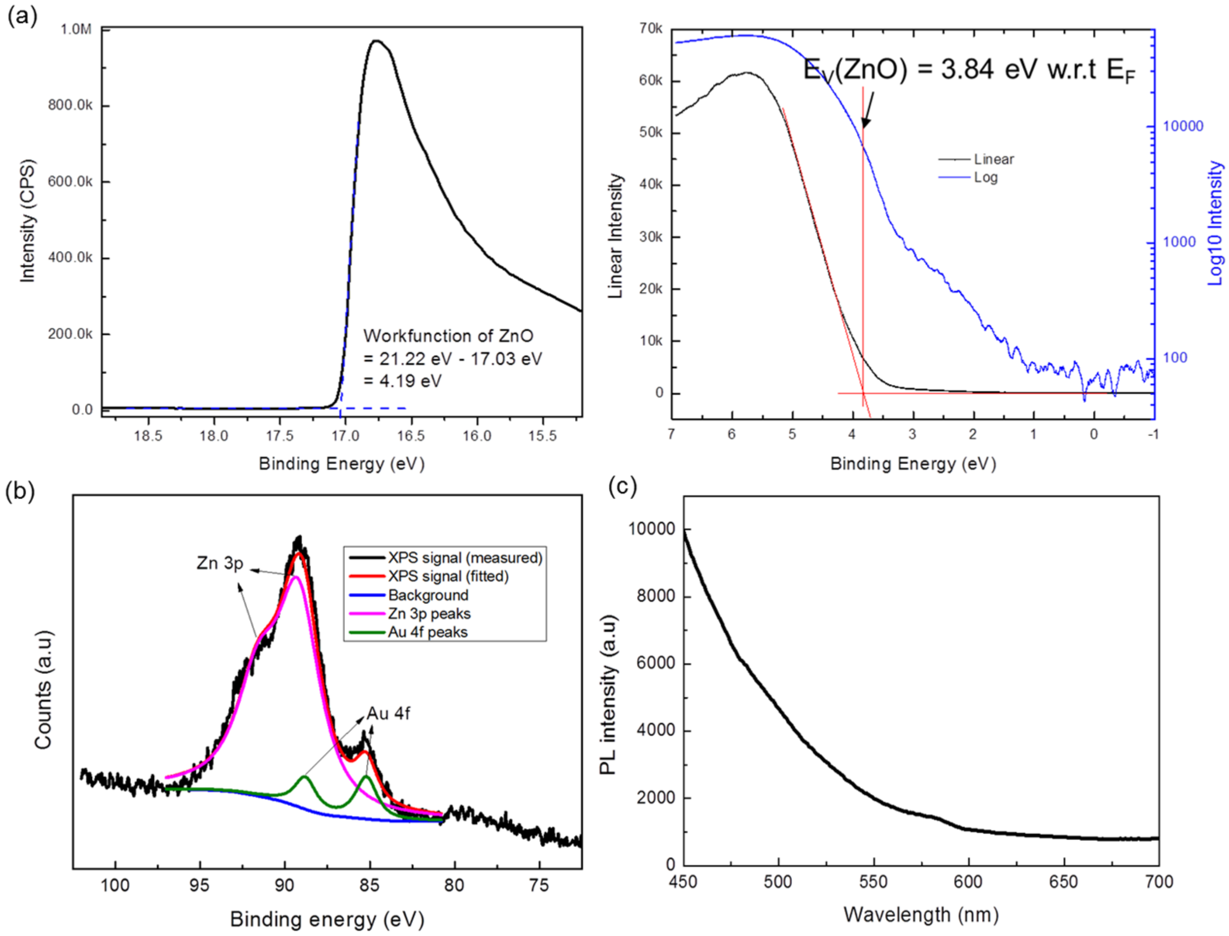

Figure S3. (a) Ultraviolet photoelectron spectroscopy (UPS) spectra (He I scan) of the solution processed ZnO film. Workfunction of 4.19 eV was derived from the secondary electron cutoff, and valence band offset from the Fermi level was measured to be 3.84 eV, indicating the n-type nature of the film. (b) X-ray photoelectron spectroscopy (XPS) spectra (Al Kα 50 eV pass energy) obtained from the 1.8:1 nanocluster on top of the ZnO layer. Retrieved signal was a convoluted version of the signals from both Zn 3p peaks from ZnO and Au 4f peaks from Au(0)@Au(I)-thiolates. (c) Photoluminescence spectrum of the ZnO film used in this work, which does not overlap with electroluminescence spectra of the devices indicating no parasitic emission from ZnO. Film PL spectrum was recorded using Hitachi F-7000 spectrophotometer, at an excitation wavelength of 365 nm.

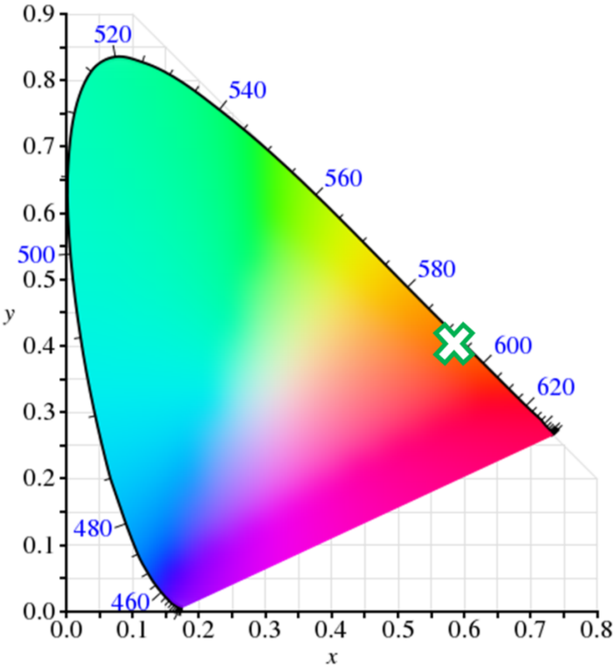

Figure S4. Commission International de l'Eclairage (CIE) 1931 chromaticity coordinates (*xy* coordinates) of the measured emission spectra from the gold nanocluster-based LEDs, which correspond well with the color of the working device (shown in the inset of Fig. 3(b)). Calculated coordinates were around (0.57-0.59, 0.40-0.41), while the dominant IR emission in the 1.2:1 ratio device did not affect the coordinate due to its non-visible nature.

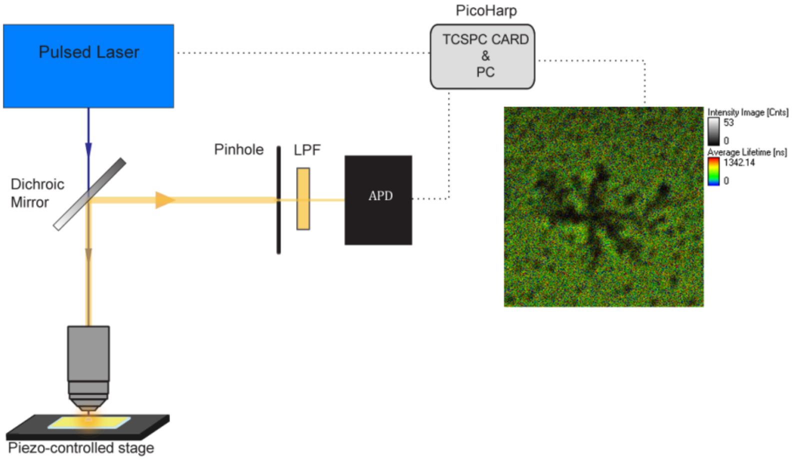

Figure S5. Simplified schematic of the fluorescence lifetime imaging microscopy (FLIM) setup